Distinct Physiologic and Inflammatory Responses Elicited in Baboons after Challenge with Shiga Toxin Type 1 or 2 from Enterohemorrhagic *Escherichia coli*[∇]

D. J. Stearns-Kurosawa,[1] Valta Collins,[1] Scott Freeman,[1]
Vernon L. Tesh,[2] and Shinichiro Kurosawa[1,3]*

Department of Pathology and Laboratory Medicine, Boston University School of Medicine, 670 Albany Street, Boston, Massachusetts[1]; Department of Microbial and Molecular Pathogenesis, Texas A&M University System Health Science Center, College Station, Texas[2]; and Department of Pathology, University of Oklahoma Health Sciences Center, Stanton Young Blvd., Oklahoma City, Oklahoma[3]

Shiga toxin-producing *Escherichia coli* is a principal source of regional outbreaks of bloody diarrhea and hemolytic-uremic syndrome in the United States and worldwide. Primary bacterial virulence factors are Shiga toxin types 1 and 2 (Stx1 and Stx2), and we performed parallel analyses of the pathophysiologies elicited by the toxins in nonhuman primate models to identify shared and unique consequences of the toxemias. After a single intravenous challenge with purified Stx1 or Stx2, baboons (*Papio*) developed thrombocytopenia, anemia, and acute renal failure with loss of glomerular function, in a dose-dependent manner. Differences in the timing and magnitude of physiologic responses were observed between the toxins. The animals were more sensitive to Stx2, with mortality at lower doses, but Stx2-induced renal injury and mortality were delayed 2 to 3 days compared to those after Stx1 challenge. Multiplex analyses of plasma inflammatory cytokines revealed similarities (macrophage chemoattractant protein 1 [MCP-1] and tumor necrosis factor alpha [TNF-α]) and differences (interleukin-6 [IL-6] and granulocyte colony-stimulating factor [G-CSF]) elicited by the toxins with respect to the mediator induced and timing of the responses. Neither toxin induced detectable levels of plasma TNF-α. To our knowledge, this is the first time that the *in vivo* consequences of the toxins have been compared in a parallel and reproducible manner in nonhuman primates, and the data show similarities to patient observations. The availability of experimental nonhuman primate models for Stx toxemias provides a reproducible platform for testing antitoxin compounds and immunotherapeutics with outcome criteria that have clinical meaning.

Infection with Shiga toxin-producing *Escherichia coli* (STEC) results in intestinal cramps and bloody diarrhea, followed 5 to 12 days later in some patients by the development of hemolytic-uremic syndrome (HUS) (16, 18). HUS is characterized clinically by the triad of thrombocytopenia, hemolytic microangiopathy, and renal injury and is the leading cause of acute renal failure in otherwise healthy children in the United States. An antibiotic regimen is not recommended, and treatment options are limited to critical care support (47). Patients with diarrhea-associated HUS can have long-term renal impairment of varying severity, and approximately one-fourth of patients have neurologic sequelae, including seizures, coma/stupor, cortical blindness, ataxia, and paraplegia (10, 14).

The natural infection route is gastrointestinal, via contaminated food or water. The bacteria colonize the intestinal lumen, with most strains forming characteristic attaching-and-effacing lesions, and the organisms may synthesize and release one or more toxins that are primary virulence factors contributing to the clinical manifestations of HUS (19). The toxins are AB_5 holotoxins, referred to as Shiga toxins due to their func-

tional and structural similarities to Shiga toxin expressed by *Shigella dysenteriae* serotype 1 (4). Shiga toxin type 1 (Stx1) is essentially identical to the *Shigella* toxin (4), differing by one amino acid, but shares only 58% amino acid identity with Shiga toxin type 2 (Stx2). Stx1 and Stx2 have distinct spatial conformations (8) and dissociation rates from receptor-lipid surfaces (24). STEC strains may secrete one or both toxins and several toxin variants, and clinical studies have demonstrated that HUS is most often associated with the expression of Stx2 (3), particularly following infection with *E. coli* O157:H7 strains (12, 20). All Shiga toxins share a cellular intoxication mechanism in which B subunits oligomerize into pentamers for interaction with a cell surface globotriaosylceramide Gb_3 (CD77) receptor. Following binding, holotoxins are internalized via clathrin-dependent or clathrin-independent mechanisms and undergo retrograde transport through the *trans*-Golgi network and Golgi apparatus to reach the endoplasmic reticulum (33, 46). During transport, the A subunit undergoes limited proteolysis, and once in the endoplasmic reticulum, a fragment of the A subunit translocates into the cytoplasm, where its *N*-glycosidase activity inactivates the 28S rRNA component of eukaryotic ribosomes to inhibit protein synthesis and cause cell death (25, 43).

While Stx1 and Stx2 share many characteristics, they are not identical and there is evidence that toxin-specific activities may be clinically relevant. Both toxins are internalized after binding

* Corresponding author. Mailing address: Department of Pathology and Laboratory Medicine, Boston University School of Medicine, 670 Albany Street, Boston, MA 02118. Phone: (617) 414-7091. Fax: (617) 414-7073. E-mail: kurosawa@bu.edu.

to Gb$_3$, but the mechanisms of their intracellular trafficking through polarized intestinal epithelial cells to reach the intestinal endothelium are very different (15). Also, endothelial sensitivities to Stx1 and Stx2 differ depending on the vascular bed, with intestinal endothelium being more sensitive to the Shiga toxins than saphenous vein endothelium (12), and glomerular endothelial cells are about 1,000 times more sensitive to Stx2 than human umbilical vein endothelial cells (17). The mechanisms for these differences are not completely understood but may be related to receptor density, toxin effects on endoplasmic reticulum stress responses and apoptosis (22, 41), or local availability of sensitizing cytokines (5, 7, 11).

Most animal models show greater sensitivity to Stx2, including murine, rabbit, and gnotobiotic piglet models, although renal and neurologic micropathologies differ from those in humans and between animal species (6, 9, 45). Earlier studies with the baboon (*Papio*) model showed that a bolus infusion of purified Stx1 induced intestinal injury, kidney glomerular injury, microangiopathic anemia, thrombocytopenia, and neurologic abnormalities similar to those in humans, suggesting that the baboon represents a promising preclinical animal model (44). A systemic inflammatory response was minimal after Stx1 challenge, but urinary tumor necrosis factor alpha (TNF-α) and interleukin-6 (IL-6) levels were consistent with local kidney inflammatory responses. Baboons were also more sensitive to Stx2 (38), but a direct comparison of the pathophysiologies elicited by the two toxins was difficult because of differing experimental designs. We sought to expand these earlier studies of baboons to identify similarities and differences elicited by Stx1 and Stx2 under reproducible experimental conditions. Given the clinical relevance of Stx2 production during STEC infection in patients, we were particularly interested in responses after Stx2 challenge, for which few data are available from the baboon model. We present the metabolic, physiologic, and inflammatory responses in baboons after intravenous challenge with Stx1 or Stx2. The observed differences in pathophysiology elicited by the two toxins may contribute to a better understanding of the differences in clinical manifestations produced by the toxins.

MATERIALS AND METHODS

Reagents. Recombinant Stx2 was obtained from BEI Resources (Manassas, VA). Purified recombinant Stx1 was prepared from cell lysates obtained from *E. coli* DH5α harboring plasmid pCKS112, which contains the *stx$_1$* operon under the control of a thermoinducible promoter (45). Stx1 was purified from cell lysates by sequential ion-exchange and chromatofocusing chromatography. The purity of toxins was assessed by SDS-PAGE with silver staining and by Western blot analysis. Prepared toxins contained <0.1 ng endotoxin per ml, as determined by *Limulus* amoebocyte lysate assay (Associates of Cape Cod, Inc., East Falmouth, MA).

Animals. *Papio cynocephalus cynocephalus* or *P. c. anubis* baboons were purchased from the Oklahoma Baboon Research Resource at the University of Oklahoma Health Sciences Center. All baboons were juvenile (1.5 to 3 years; 6 to 8 kg), before sexual maturation, were outbred and free of tuberculosis, and had leukocyte concentrations of <15,000/mm^3. The animals were housed and used in accordance with the guidelines and approved protocols of the institutional animal care and use committees and the institutional biosafety committees of Boston University School of Medicine and the University of Oklahoma Health Sciences Center.

Toxin challenge procedures. The animal studies were performed at the University of Oklahoma Health Sciences Center animal annex, using previously published procedures (42, 44). Briefly, baboons were fasted overnight before the study, with free access to water. They were sedated the morning of the experi-

ment by use of ketamine (10 mg/kg of body weight, given intramuscularly [i.m.]) and were orally intubated. Anesthesia was maintained using sodium pentobarbital (5 to 10 mg/kg for maintenance) as deemed necessary by monitoring the eyelid reflex. An indwelling catheter was placed in the forearm cephalic vein for bolus infusion of toxin (1 to 2 ml). A second catheter was inserted into the femoral vein by venous cutdown and secured subcutaneously by an internal injection cap (Braun), where it remained for the rest of the study period and was used for blood draws, infusion of saline to replace insensible loss, central venous pressure (CVP) monitoring, and anesthesia. Death is not an end point for these studies, and baboons were euthanized according to established criteria if deemed necessary before the end of the 7-day experimental period. At necropsy, the gross pathology of the organs was examined and tissues were harvested for archiving. All animals received enrofloxacin (Baytril; 10 mg/kg i.m.) prior to cutdown and catheter placement on day 0. Baboons then received either prophylactic levofloxacin (Levaquin; 3.5 mg/kg as an intravenous [i.v.] bolus) or enrofloxacin (10 mg/kg i.m.) each day over the experimental period.

Animals were weighed daily, and toxin-induced hypovolemia was controlled based on criteria developed in previous studies (44). Replacement of fluids with saline (no more than three bolus infusions of 10 ml/kg) was done according to the following criteria: (i) if weight is less than that at time zero (T0), then infuse sufficient normal saline to return animal to initial weight (1 g = 1 ml) at 1 ml/kg/min; (ii) if mean arterial pressure is <70 mm Hg, then infuse normal saline (10 ml/kg at 1 ml/kg/min), repeating as needed, while following CVP and mean systemic arterial pressure (MSAP) and stopping when MSAP is >70 mm Hg, or sooner if the CVP is >10 cm H$_2$O; (iii) if CVP is <3 cm H$_2$O, then infuse normal saline and repeat as needed to raise the CVP to >3 cm H$_2$O; and (iv) if urine output is <2 ml/kg/h, but weight, MSAP, and CVP are not low, then infuse saline and repeat as needed or until the CVP is >10 cm H$_2$O.

Hematology, clinical chemistry, and urine analyses. Blood samples were obtained at T0 (before toxin challenge), eight times during the first 24 h, and daily thereafter. Complete blood counts (CBCs) were determined with a Horiba ABX Micros 60 hematology analyzer (Horiba, Irvine, CA). Blood smears were stained with Wright's stain, and schistocyte counts were determined as percentages of 200 red blood cells. A Foley catheter (6 French units, 30 cm, 1.5-ml balloon; Rusch, Research Triangle Park, NC) was inserted for urine collection. The animals were all similar in size (body surface area); urine was collected on day 0 before toxin challenge for 60 min and on subsequent days for 20 min. Urinalysis was obtained using dipsticks (Multistix 10SG) on samples collected before saline infusion if indicated to correct for hypovolemia. Blood urea nitrogen (BUN) and creatinine levels were determined on citrated plasma by standard clinical chemistry analyses (Veterinary Associates Laboratory, Edmond, OK). Activated partial thromboplastin times (APTT) were determined on citrated plasma by use of a KC4 coagulation analyzer (Trinity Biotech, Wickland, Ireland) and TriniCLOT automated APTT reagent (Trinity Biotech). The APTT tests for all factors in the intrinsic coagulation pathway, including factors II, V, VIII, IX, X, XI, and XII, and is independent of platelet counts. Fibrinogen levels were determined by reference to a standard curve, using a KC4 coagulation analyzer. For the standard curve, bovine thrombin was added to a reference plasma of known fibrinogen content, and the clotting time was inversely proportional to the fibrinogen content. The fibrinogen level at T0 for the 21 animals in this study was 141.8 ± 40.6 mg/dl (mean ± standard deviation [SD]).

Cytokine analyses. Cytokine protein levels were quantified by xMAP multiplex fluorescent bead-based assays, using a Luminex 200 IS system (Millipore, Billerica, MA), Luminex xPONENT software (Luminex, Austin, TX), and nonhuman primate cytokine panel kits (Millipore), which provide the beads, buffers, and detection reagents. Samples were thawed, diluted as appropriate, and incubated with beads for 2 h at room temperature with vigorous mixing. Samples were washed twice with vacuum filtration and incubated with biotin-conjugated antibodies selective for each biomarker for 1 h at room temperature. Phycoerythrin-conjugated streptavidin was added, and samples were incubated for 30 min at room temperature, followed by washing. Beads were resuspended in 150 µl sheath fluid, and samples were assayed on a Luminex 200 system. Standard curves for each biomarker ranged from 0 to 10,000 pg/ml. Samples with values of >9,000 pg/ml were diluted appropriately and reanalyzed. For each sample, the median fluorescence intensity was analyzed with a weighted 5-parameter logistic (Milliplex Analyst; Millipore) and quantified relative to the standard curve for that cytokine. Differences from baseline values were analyzed by paired Student's *t* test, and *P* values of <0.05 were considered significant.
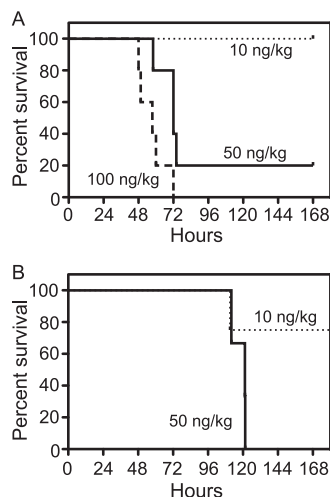
FIG. 1. Baboons are more sensitive to Stx2, but with a delayed time course. Baboons were challenged with an i.v. bolus of Stx1 (A) or Stx2 (B) in sterile saline, and animals were monitored over a 7-day period. Animals were challenged with toxin at 10 ng/kg (dotted line), 50 ng/kg (solid line), or 100 ng/kg (dashed line). A total of 21 animals were challenged with either Stx1 at the three doses (n = 3, 5, and 5) or Stx2 at two doses (n = 4 and 4).
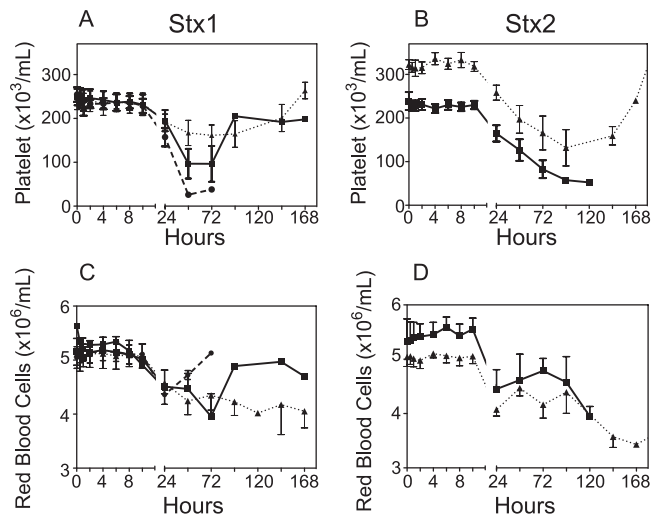

FIG. 2. Thrombocytopenia and anemia result after toxin challenge. Changes in platelet (A and B) and red blood cell (C and D) counts were determined at the indicated time points after challenge with 10 ng/kg (▲), 50 ng/kg (■), or 100 ng/kg (●) Stx1 or Stx2. Data shown are means ± SD.

RESULTS

Survival. Anesthetized baboons were challenged with a single intravenous bolus injection of recombinant, purified Stx1 or Stx2 at different doses. Blood was taken just before toxin challenge (T0), followed by sampling at defined periods thereafter. Survival after challenge with 10, 50, or 100 ng/kg Stx1 was dose dependent (Fig. 1A), with the highest dose lethal for all animals, with mortality by day 2 or 3. All animals challenged with 10 ng/kg Stx1 (n = 3) survived. The 50-ng/kg Stx1 dose (n = 5) was more severe, but one animal eventually recovered, and the 100-ng/kg Stx1 dose (n = 5) was lethal. Baboons were more sensitive to Stx2, in that 3 of 4 animals challenged with 10 ng/kg Stx2 were survivors, but challenge with 50 ng/kg Stx2 (n = 4) was lethal, though mortality was delayed until day 4 or 5 (Fig. 1B). Median survival times at the lethal dose were different (57.5 h for Stx1 and 121.3 h for Stx2; log rank [Mantel-Cox] test). The animals died at a much lower dose of Stx2, but the time to death was longer. For survivors, there were no changes in symptoms or mortality after this 7-day period. Several surviving baboons were monitored for 28 days, with no persistent or emerging clinical signs, and appeared to be fully recovered.

Hematology. Complete blood counts performed on blood samples at each time point showed a progressive loss of circulating platelets after challenge with Stx1 or Stx2 (Fig. 2). The extent of thrombocytopenia was dose dependent, with recovery of cell counts if the animal received a low dose or was recovering. Compared to Stx1 challenge, a more gradual development of thrombocytopenia with time was observed after Stx2 challenge (Fig. 2A and B). Animals developed anemia after challenge with either toxin, with a gradual decline in red blood cell counts (Fig. 2C and D) that was reflected in significant declines in hematocrit (Table 1). In general, white blood cell counts did not change (Table 1), with the exception of low-dose Stx1-challenged animals, who had elevated white cell

counts at 24 and 48 h, probably reflecting an acute-phase response. Examination of blood smears obtained at euthanasia or on day 6 or 7 revealed schistocytes (fragmented red blood cells) in toxin-challenged animals (Table 1). Although platelet levels declined, consumptive coagulopathy or disseminated intravascular coagulation was not evident because APTT were prolonged modestly only after 24 to 48 h and fibrinogen levels remained steady for several days, actually increasing during the acute-phase response (Fig. 3).

Acute renal failure. Renal damage was a consequence of challenge with either Stx1 or Stx2. Urine output decreased in both toxin-challenged groups in the first 24 h, essentially ceasing at the high doses (Fig. 4A and B). Proteinuria, indicative of glomerular damage and a loss of filtration function, was dose dependent for both toxins but more sensitive to Stx2 (Fig. 4C and D). Increases in plasma BUN and creatinine by 24 to 48 h paralleled the onset of kidney damage after challenge with either toxin (Fig. 5). The levels returned to baseline after low-dose toxin challenge or if the responses were compensated and the animal was recovering. Most animals showed physical signs of edema by 24 to 48 h, with swelling of the face and abdomen, which resolved within a day or two in the low-dose-challenged animals. However, despite frequent monitoring and fluid support to maintain central venous pressure, animals who received the higher toxin doses had progressive loss of kidney function and thrombocytopenia leading to death. Gross pathology observations of the kidneys at necropsy on day 2 (48 h) after challenge with a 100-ng/kg Stx1 lethal dose revealed mild to moderate congestion at the cortico-medullary junction (Fig. 6B). In contrast, the 50-ng/kg Stx2 lethal dose resulted in severe medullary congestion and marked cortical ischemia at necropsy on day 5 (121.6 h) postchallenge (Fig. 6C).

Systemic inflammation. Quantification of circulating proinflammatory biomarkers revealed a systemic inflammatory response with shared and unique features depending on the toxin challenge. Interleukin-6 (IL-6) and monocyte chemoattractant

TABLE 1. Hematology changes 24 h after toxin challenge[a]

Toxin	Dose (ng/kg)	Hematocrit (%)	WBC count (cells/nl)	Schistocytes (%)[b]
Stx1	10	34.6 ± 3.1 (32.5–38.1)*	17.4 ± 5.5 (12.5–23.3)***	1.8 ± 0.3 (1.5–2)
	50	33.0 ± 3.5 (27–35.4)**	7.7 ± 2.4 (4.5–10.2)	6.3 ± 3.5 (0.5–9)
	100	31.3 ± 2.7 (27.6–34.8)***	6.9 ± 2.8 (4.4–10.5)	3.8 ± 3.0 (1.5–9)
Stx2	10	30.9 ± 0.9 (29.5–31.8)***	9.2 ± 2.8 (6.8–13.1)	3.1 ± 4.9 (0–10.5)
	50	31.0 ± 5.5 (25.3–36.7)**	10.6 ± 2.0 (8.4–10.7)	4.0 ± 1.8 (1.5–5.5)
None[c]	0	38.3 ± 2.9 (33–45)	7.6 ± 2.5 (3.1–11.1)	0.8 ± 0.9 (0–3.0)

[a] Data are means ± SD (ranges). *, $P = 0.05$; **, $P < 0.001$; ***, $P < 0.0001$ compared to group prior to challenge (Student's t test).
[b] Percentage at euthanasia, or on day 6 or 7 for long-term survivors.
[c] T0 data before challenge for all animals in the study ($n = 21$).

protein 1 (MCP-1) are global markers of systemic inflammation that predict outcomes in patients and animal models of bacterial sepsis (21, 28, 31), and increases were observed in baboons after challenge with the toxins (Fig. 7A to D). Notably, different response patterns could be observed between the two toxins. The early and sustained rise in IL-6 after Stx1 challenge, from 4 to 24 h, was not observed in the Stx2-challenged baboons, although the sharp rise in IL-6 levels in the high-dose groups (100 ng/kg Stx1 and 50 ng/kg Stx2) just before death was a shared response. A significant difference from baseline IL-6 levels was observed by 30 min after challenge with 50 or 100 ng/kg Stx1 ($P < 0.01$). At the high Stx1 dose, elevated IL-6 levels persisted, with differences from baseline at 6 to 8 h ($P < 0.01$) and 10 h ($P < 0.001$). Increases in MCP-1 levels occurred similarly 24 to 48 h after Stx1 or Stx2 challenge, in a dose-dependent fashion (Fig. 7C and D), although the rise was more gradual after Stx2 challenge. Granulocyte colony-stimulating factor (G-CSF) increased within 1 h ($P = 0.05$; $P < 0.05$ after 4 h) after challenge with 100 ng/kg Stx1, with sustained rises over several days with the 50- and 100-ng/kg Stx1

doses. In contrast, little G-CSF was induced after Stx2 challenge, even with the 50-ng/kg dose that otherwise elicited severe responses in the baboons (Fig. 7E and F). Baboon tumor necrosis factor alpha (TNF-α) was not detected in plasma after challenge with either toxin (Fig. 7G and H), consistent with previous observations in the baboon Stx1 model obtained with a different antibody-based assay (44). There were either no changes or no detectable levels of granulocyte-macrophage colony-stimulating factor (GM-CSF), IL-1β, IL-2, IL-4, IL-12/23, IL-13, IL-17, IL-18, gamma interferon (IFN-γ), and macrophage inflammatory protein 1β (MIP-1β).

DISCUSSION

The availability of the baboon Stx1 and Stx2 toxemia models permits parallel analyses of shared and unique responses elicited by the toxins in a near-human setting. The major observations from this study are that a single bolus injection of Stx1 or Stx2 induced shared responses of thrombocytopenia, anemia, and acute renal failure in baboons, but there were distinct
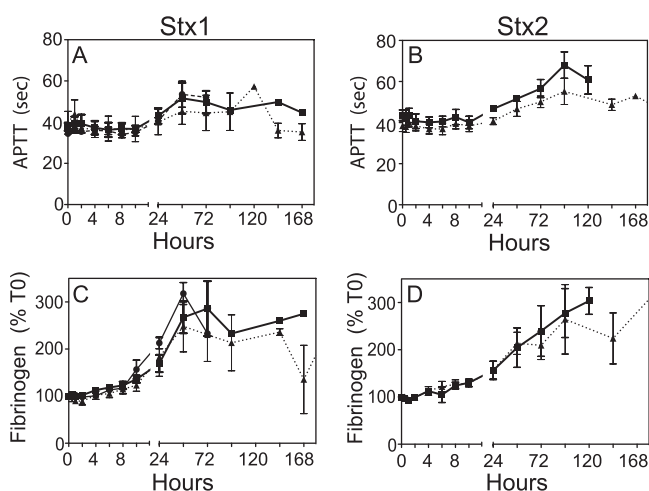

FIG. 3. Consumptive coagulopathy was not present during the disease course. The APTT (A and B), which are not dependent on platelet counts, were steady or modestly prolonged several days after Stx1 or Stx2 challenge. Fibrinogen levels (C and D) are shown as a percentage of the T0 value for each animal. The absolute fibrinogen level at T0 before challenge was 141.8 ± 40.6 mg/dl ($n = 21$). The symbols for toxin doses are the same as those in Fig. 2. Data shown are means ± SD.
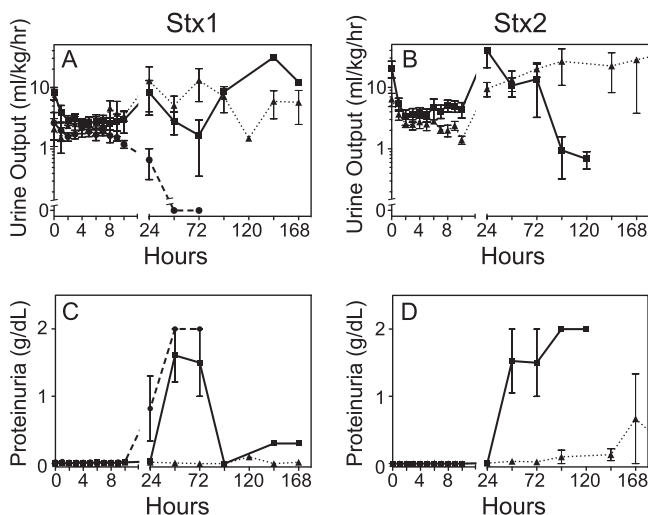

FIG. 4. Progressive loss of renal function after Stx1 or Stx2 challenge. Urine output (A and B) was measured in all animals, using samples collected at the indicated time points. Data shown are for urines collected before saline infusion to correct for hypovolemia, as defined in Materials and Methods. Proteinuria (C and D) was determined by dipstick measurements immediately after collection. Data shown are means ± SD.
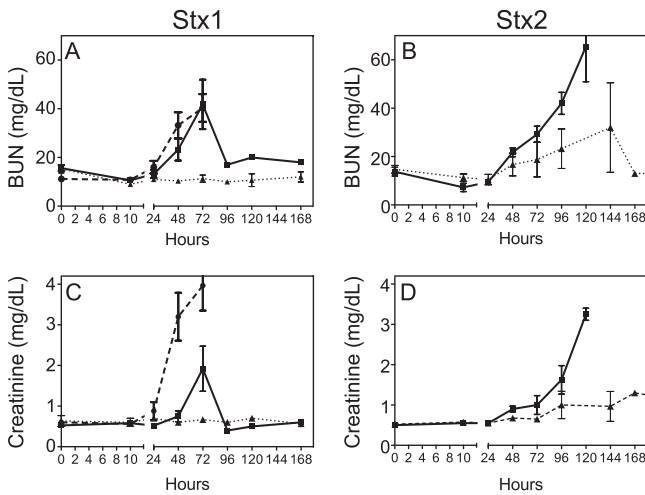
FIG. 5. Acute renal failure occurs after challenge with either toxin but is delayed by 2 to 3 days after Stx2 challenge. BUN (A and B) and creatinine (C and D) levels were determined in citrated plasma samples taken at the indicated time points. The symbols for toxin doses are the same as those in Fig. 2. Data shown are means ± SD.

differences in the timing and magnitude of responses elicited by the two toxins. Furthermore, although both toxins induced a systemic inflammatory response, the cytokine patterns induced were distinct between the toxins, with differences in the mediators induced as well as in the timing and magnitude of the responses.

We showed that both toxins alter hematologic parameters and target the kidneys, with resulting thrombocytopenia, anemia, red blood cell fragmentation, progressive anuria, proteinuria, and reduced glomerular function. In patients, complete HUS has been defined as having platelet counts of <150,000/μl, a hematocrit of <30% with evidence of intravascular hemolysis, and a BUN level of >20 mg/dl, and incomplete HUS is defined as having two of these criteria (2). The hematologic
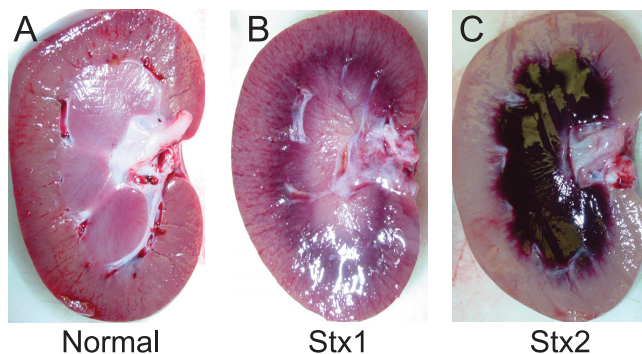

FIG. 6. Kidney gross pathology observations at necropsy. The organ appearance of a kidney from an unchallenged baboon of approximately the same age (A) is compared with those from a baboon euthanized 48 h after challenge with 50 ng/kg Stx1 (B) and a baboon euthanized 121.6 h after challenge with 100 ng/kg Stx2 (C). Both toxin-challenged animals had acute renal failure, as judged by reduced urine output and proteinurea and increased plasma BUN and creatinine levels. The gross pathology differences between Stx1 and Stx2 shown are representative of all animals in the high-dose (100 ng/kg Stx1 and 50 ng/kg Stx2) groups.
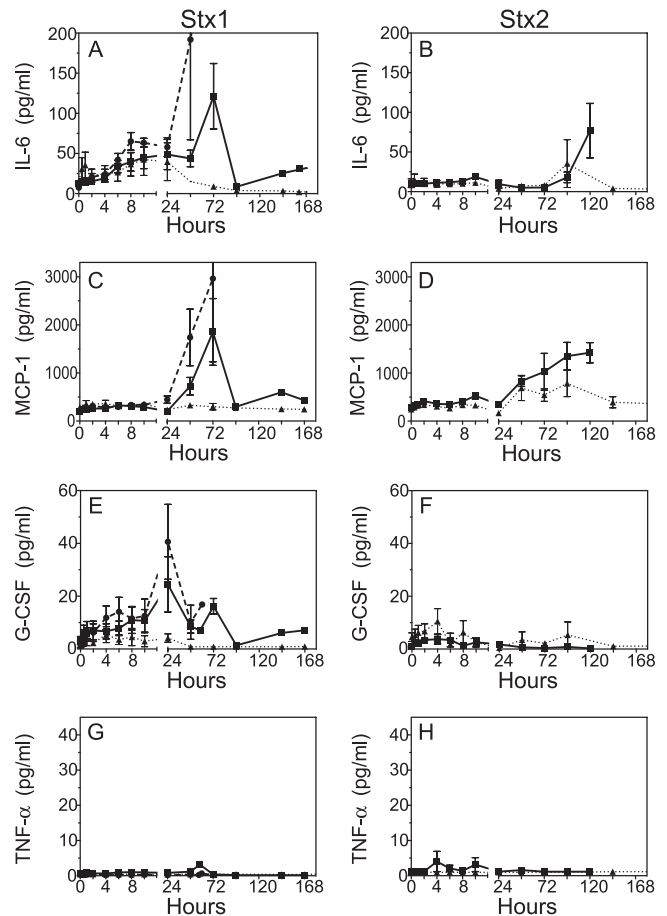

FIG. 7. Stx1 and Stx2 challenges result in distinct inflammatory response patterns. Biomarkers were measured in citrated plasma samples after challenge with 10 ng/kg (▲), 50 ng/kg (■), or 100 ng/kg (●; Stx1 only) toxin, using a multiplex bead-based assay designed for quantification of nonhuman primate antigens. Dose-dependent changes in the proinflammatory mediators IL-6 (A and B), MCP-1 (C and D), and G-CSF (E and F) are shown as means ± SD. (G and H) Neither toxin stimulated production of circulating TNF-α. Paired t tests were used to determine statistical differences from baseline for the following early biomarker changes: IL-6 at 100 ng/kg Stx1 ($P < 0.01$ at 0.5, 2, 6, and 8 h; $P < 0.05$ at 4 h; and $P < 0.001$ at 10 h) and 50 ng/kg Stx1 ($P < 0.01$ at 0.5 h and $P < 0.05$ at 4, 6, 8, and 10 h) and G-CSF at 100 ng/kg Stx1 ($P \leq 0.05$ at 4, 6, 8, and 10 h).

and renal function changes observed in the baboons after a single-dose challenge with Stx1 or Stx2 were similar to those observed in patients.

Differences in the physiologic responses elicited by the toxins in the baboons were largely in their timing. While the absolute losses of platelet counts were similar, a high dose of Stx1 resulted in fairly abrupt thrombocytopenia by 24 to 48 h, whereas the loss of platelets after Stx2 challenge was through a gradual daily decrease until either euthanasia at day 4 or 5 or resolution and recovery. Differences in renal gross pathology may also be attributable to the timing of organ injury. In the kidney, the cortico-medullary congestion noted on day 2 after high-dose Stx1 challenge may progress to the severe medullary congestion seen on day 5 after Stx2 challenge. While it is possible that the far more severe renal lesions after high-dose

Stx2 challenge represent toxin specificity, it is also possible that the additional 2 to 3 days to euthanasia and necropsy allowed more time for the pathology to develop. It is notable that anemia developed after exposure to either toxin, and red cell counts continued to decrease and remained low even when markers of renal function and inflammation were resolving after low-dose toxin challenge and the animal appeared to be recovering. Patients with STEC-induced HUS can become profoundly anemic and require transfusions (16).

The shorter, 2- to 3-day survival time with a lethal dose of Stx1 (100 ng/kg; median time to death, 57.5 h) than the 4- to 5-day survival time after a lethal dose of Stx2 (50 ng/kg; median time to death, 121.3 h) demonstrated a higher sensitivity to Stx2 but a longer time to severe organ injury and death. More-rapid kidney injury by Stx1 is supported by the observations that BUN and creatinine levels increased more acutely and urine output dropped more rapidly and to a greater degree in the Stx1-challenged animals. We do not interpret this to mean that Stx1 preferentially targets the kidney, but rather that there may be differences in toxin dissemination or processing *in vivo* that could contribute to delayed Stx2 renal injury. The molecular basis for delayed organ damage and mortality after Stx2 remains enigmatic, because both toxins require the Gb_3 (CD77) receptor for cell intoxication (27), although they bind with slightly different kinetics and affinities (17, 24). Using the gnotobiotic piglet model and isogenic *E. coli* strains with similar toxin production capabilities, Donohue-Rolfe et al. showed that oral challenge with strains expressing Stx2 alone induced more neurologic symptoms than did challenge with strains that express only Stx1 (6, 37). This also supports the notion that the toxins can induce different systemic pathophysiologies. With respect to timing differences, the current experimental baboon observations are reminiscent of clinical observations in which renal injury in young children correlates with Stx2 production from STEC and the development of hemolytic-uremic syndrome is delayed by an average of 6 days after infection (2).

Measurement of circulating biomarkers by bead-based multiplex assays revealed unexpected differences in the proinflammatory cytokines induced by Stx1 and Stx2, with differences in the mediator induced as well as in the timing and magnitude of the response. From a broad perspective, Stx1 appeared to induce a stronger systemic inflammatory response in the baboons, as judged by more cytokines being induced, and at higher levels. Though they are present in the circulation, a role for these mediators in disease severity, outcome, or prognosis cannot be inferred from the current study. An inflammatory response is well documented for pediatric patients with STEC infection, who have elevated IL-6, IL-10, IL-1Ra, G-CSF, and chemokine levels (29, 30) and may (23) or may not (30) have elevated plasma TNF-α levels. In the baboons, IL-6 and MCP-1 levels were induced to similar levels after either toxin and were dose dependent, but Stx2-induced responses were more gradual and were delayed by several days. In contrast, changes in G-CSF were very different between the toxins. Stx1 challenge increased circulating G-CSF levels, particularly at the 50- and 100-ng/kg doses, whereas G-CSF was only minimally increased early after Stx2 challenge, regardless of the toxin dose. To our knowledge, Stx toxin-specific changes in plasma cytokines have not been studied in parallel in other animal models, and the baboon data suggest that the toxins

may exert independent influences on cytokine mRNA stability and/or gene transcription in susceptible cells. Increased G-CSF levels would be expected to result in increased white cell counts, but this did not occur, nor did differential cell counts change (not shown). In fact, the animals challenged with 10 ng/kg Stx1 paradoxically had the highest white cell counts and the lowest plasma G-CSF levels. G-CSF production is tightly regulated at both the translational and posttranslational levels, and stabilization of mRNA is observed as a result of multiple mediators, including IL-4, TNF-α, and IFN-γ (1). However, these mediators were not observed in the baboons, at least not systemically. In mice, Stx1 localizes to the bone marrow of the spine, long bones, and ribs (34), and it is possible that even though peripheral cells may produce G-CSF, its biological activity at the bone marrow may be inefficient or blocked. The distribution of toxins in patients or nonhuman primates is not known, and studies are in progress to understand the molecular basis and biologic significance of the cytokine responses unique to each toxin.

We did not detect plasma TNF-α in any of the baboons after challenge with either toxin, even at high doses, consistent with previous Stx1 studies of the baboon model (40, 44). TNF-α is a well-known early proinflammatory mediator of bacterial sepsis in patients and most animal models, including baboons (13, 26, 42). In contrast, mice have elevated plasma TNF-α and kidney TNF-α mRNA after multiple Stx2 injections that induce thrombocytopenia and renal injury (36), and cultured cells will undergo TNF-α transcription and protein release after Stx1 intoxication under lipopolysaccharide (LPS)-free conditions (35). These differences may be species dependent, or TNF-α production may rely on a balance of gene transcription induced by other local mediators despite toxin-induced pressures to undergo cellular apoptosis (22, 41).

While there are parallels between the current baboon results and patient observations, the current study models are most accurately viewed as nonhuman primate models of toxemia, not STEC infection, where the pathogen is bacterial and the infection route is gastrointestinal. Furthermore, the toxins were administered as a bolus challenge rather than as repeated or intermittent toxin exposures, as would be expected during an intestinal bacterial infection. We observed increased white cell counts only after low-dose Stx1 challenge, whereas in patients with STEC infection, a white cell count of >10,500/μl is associated with a 5-fold-increased risk of HUS (2). It is reasonable to expect that patients infected with STEC will be exposed to a variety of bacterial factors and that possible breaching of the gut epithelial barrier due to injury will exacerbate the insult, providing exposure to LPS from commensal flora. In an earlier baboon Stx1 study, LPS and Stx1 coadministration resulted in more-severe kidney damage in response to an otherwise subtoxic challenge (39). This is underscored by studies which demonstrated the importance of other bacterial molecules necessary for epithelial attachment in the gut and the interplay between the toxins, bacterial colonization, and inflammation that give rise to systemic disease (3, 32).

Ongoing studies in our laboratory continue to characterize the baboon toxemia models with respect to inflammation, pathology, and neurologic abnormalities to further advance our understanding of how the toxins exert their influence at the organ and cellular levels. The current nonhuman primate mod-

els of Stx1 and Stx2 toxemia provide a platform for reproducible testing of immunotherapeutics and antitoxin compounds in a near-human setting, with definable outcomes that have clinical meaning. With the baboon models, it should be possible to test therapeutics tailored to one or both toxins and to independently judge effects on toxin-specific responses. In this way, it may be possible to more rapidly develop and advance therapeutics for STEC infection for a clinical setting in which patients may present with STEC strains that secrete different ratios of toxins.

ACKNOWLEDGMENTS

REFERENCES

1. **Barreda, D. R., P. C. Hanington, and M. Belosevic.** 2004. Regulation of myeloid development and function by colony stimulating factors. Dev. Comp. Immunol. **28:**509–554.
2. **Bell, B. P., P. M. Griffin, P. Lozano, D. L. Christie, J. M. Kobayashi, and P. I. Tarr.** 1997. Predictors of hemolytic uremic syndrome in children during a large outbreak of Escherichia coli O157:H7 infections. Pediatrics **100:**E12.
3. **Boerlin, P., S. A. McEwen, F. Boerlin-Petzold, J. B. Wilson, R. P. Johnson, and C. L. Gyles.** 1999. Associations between virulence factors of Shiga toxin-producing Escherichia coli and disease in humans. J. Clin. Microbiol. **37:**497–503.
4. **Calderwood, S. B., F. Auclair, A. Donohue-Rolfe, G. T. Keusch, and J. J. Mekalanos.** 1987. Nucleotide sequence of the Shiga-like toxin genes of Escherichia coli. Proc. Natl. Acad. Sci. **84:**4364–4368.
5. **Clayton, F., T. J. Pysher, R. Lou, D. E. Kohan, N. D. Denkers, V. L. Tesh, F. B. Taylor, Jr., and R. L. Siegler.** 2005. Lipopolysaccharide upregulates renal Shiga toxin receptors in a primate model of hemolytic uremic syndrome. Am. J. Nephrol. **25:**536–540.
6. **Donohue-Rolfe, A., I. Kondova, S. Oswald, D. Hutto, and S. Tzipori.** 2000. Escherichia coli O157:H7 strains that express Shiga toxin (Stx) 2 alone are more neurotropic for gnotobiotic piglets than are isotypes producing only Stx1 or both Stx1 and Stx2. J. Infect. Dis. **181:**1825–1829.
7. **Ergonul, Z., and A. K. Hughes, and D. E. Kohan.** 2003. Induction of apoptosis of human brain microvascular endothelial cells by Shiga toxin 1. J. Infect. Dis. **187:**154–158.
8. **Fraser, M. E., M. Fujinaga, M. M. Cherney, A. R. Melton-Celsa, E. M. Twiddy, A. D. O'Brien, and M. N. G. James.** 2004. Structure of Shiga toxin type 2 (Stx2) from Escherichia coli O157:H7. J. Biol. Chem. **279:**27511–27517.
9. **Garcia, A., C. J. Bosques, J. S. Wishnok, Y. Feng, B. J. Karalius, J. R. Butterton, D. B. Schauer, A. B. Rogers, and J. G. Fox.** 2006. Renal injury is a consistent finding in Dutch belted rabbits experimentally infected with enterohemorrhagic Escherichia coli. J. Infect. Dis. **193:**1125–1134.
10. **Garg, A. X., R. S. Suri, N. Barrowman, F. Rehman, D. Matsell, M. P. Rosas-Arellano, M. Salvadori, R. B. Haynes, and W. F. Clark.** 2003. Long-term renal prognosis of diarrhea-associated hemolytic uremic syndrome: a systematic review, meta-analysis, and meta-regression. JAMA **290:**1360–1370.
11. **Harrison, L. M., C. van den Hoogen, W. C. van Haaften, and V. L. Tesh.** 2005. Chemokine expression in the monocytic cell line THP-1 in response to purified Shiga toxin 1 and/or lipopolysaccharides. Infect. Immun. **73:**403–412.
12. **Hedican, E. B., C. Medus, J. M. Besser, B. A. Juni, B. Koziol, C. Taylor, and K. E. Smith.** 2009. Characteristics of O157 versus non-O157 Shiga toxin-producing Escherichia coli infections in Minnesota, 2000–2006. Clin. Infect. Dis. **49:**358–364.
13. **Hinshaw, L. B., P. Tekamp-Olson, A. C. Chang, P. A. Lee, F. B. Taylor, Jr., C. K. Murray, G. T. Peer, T. E. Emerson, Jr., R. B. Passey, and G. C. Kuo.** 1990. Survival of primates in LD100 septic shock following therapy with antibody to tumor necrosis factor (TNF alpha). Circ. Shock **30:**279–292.
14. **Hughes, D. A., T. J. Beattie, and A. V. Murphy.** 1991. Haemolytic uraemic syndrome: 17 years' experience in a Scottish paediatric renal unit. Scott. Med. J. **36:**9–12.
15. **Hurley, B. P., M. Jacewicz, C. M. Thorpe, L. L. Lincicome, A. J. King, G. T. Keusch, and D. W. K. Acheson.** 1999. Shiga toxins 1 and 2 translocate differently across polarized intestinal epithelial cells. Infect. Immun. **67:**6670–6677.
16. **Iijima, K., I. Kamioka, and K. Nozu.** 2008. Management of diarrhea-associated hemolytic uremic syndrome in children. Clin. Exp. Nephrol. **12:**16–19.
17. **Jacewicz, M. S., D. W. K. Acheson, D. G. Binion, G. A. West, L. L. Lincicome, C. Fiocchi, and G. T. Keusch.** 1999. Responses of human intestinal microvascular endothelial cells to Shiga toxins 1 and 2 and pathogenesis of hemorrhagic colitis. Infect. Immun. **67:**1439–1444.
18. **Karch, H., P. I. Tarr, and M. Bielaszewska.** 2005. Enterohaemorrhagic Escherichia coli in human medicine. Int. J. Med. Microbiol. **295:**405–418.
19. **Karmali, M. A., M. Petric, C. Lim, P. C. Fleming, G. S. Arbus, and H. Lior.** 1985. The association between idiopathic hemolytic uremic syndrome and infection by verotoxin-producing Escherichia coli. J. Infect. Dis. **151:**775–782.
20. **Kawano, K., M. Okada, T. Haga, K. Maeda, and Y. Goto.** 2008. Relationship between pathogenicity and stx genotype in Shiga toxin-producing Escherichia coli serotype O157. Eur. J. Clin. Microbiol. Infect. Dis. **27:**227–232.
21. **Kinasewitz, G. T., S. B. Yan, B. Basson, P. Comp, J. A. Russell, A. Cariou, S. L. Um, B. Utterback, P. F. Laterre, J. F. Dhainaut, and P. S. S. Group.** 2004. Universal changes in biomarkers of coagulation and inflammation occur in patients with severe sepsis, regardless of causative microorganism [ISRCTN74215569]. Crit. Care **8:**R82–R90.
22. **Lee, S.-Y., M.-S. Lee, R. P. Cherla, and V. L. Tesh.** 2008. Shiga toxin 1 induces apoptosis through the endoplasmic reticulum stress response in human monocytic cells. Cell. Microbiol. **10:**770–780.
23. **Lopez, E. L., M. M. Contrini, S. Devoto, M. F. de Rosa, M. G. Grana, M. H. Genero, C. Canepa, H. F. Gomez, and T. G. Cleary.** 1995. Tumor necrosis factor concentrations in hemolytic uremic syndrome patients and children with bloody diarrhea in Argentina. Pediatr. Infect. Dis. J. **14:**594–598.
24. **Nakajima, H., N. Kiyokawa, Y. U. Katagiri, T. Taguchi, T. Suzuki, T. Sekino, K. Mimori, T. Ebata, M. Saito, H. Nakao, T. Takeda, and J. Fujimoto.** 2001. Kinetic analysis of binding between Shiga toxin and receptor glycolipid Gb3Cer by surface plasmon resonance. J. Biol. Chem. **276:**42915–42922.
25. **O'Brien, A. D., V. L. Tesh, A. Donohue-Rolfe, M. P. Jackson, S. Olsnes, K. Sandvig, A. A. Lindberg, and G. T. Keusch.** 1992. Shiga toxin: biochemistry, genetics, mode of action, and role in pathogenesis. Curr. Top. Microbiol. Immunol. **180:**65–94.
26. **Oettinger, C. W., M. J. Souza, N. Akhavein, G. T. Peer, F. B. Taylor, and G. T. Kinasewitz.** 2007. Pro-inflammatory cytokine inhibition in the primate using microencapsulated antisense oligomers to NF-κB. J. Microencapsul. **24:**337–348.
27. **Okuda, T., N. Tokuda, S. I. Numata, M. Ito, M. Ohta, K. Kawamura, J. Wiels, T. Urano, O. Tajima, K. Furukawa, and K. Furukawa.** 2006. Targeted disruption of Gb3/CD77 synthase gene resulted in the complete deletion of globo-series glycosphingolipids and loss of sensitivity to verotoxins. J. Biol. Chem. **281:**10230–10235.
28. **Osuchowski, M. F., K. Welch, H. Yang, J. Siddiqui, and D. G. Remick.** 2007. Chronic sepsis mortality characterized by an individualized inflammatory response. J. Immunol. **179:**623–630.
29. **Proulx, F., B. Toledano, V. Phan, M. J. Clermont, M. M. Mariscalco, and E. G. Seidman.** 2002. Circulating granulocyte colony-stimulating factor, C-X-C, and C-C chemokines in children with Escherichia coli O157:H7 associated hemolytic uremic syndrome. Pediatr. Res. **52:**928–934.
30. **Proulx, F., J. P. Turgeon, C. Litalien, M. M. Mariscalco, P. Robitaille, and E. Seidman.** 1998. Inflammatory mediators in Escherichia coli O157:H7 hemorrhagic colitis and hemolytic-uremic syndrome. Pediatr. Infect. Dis. J. **17:**899–904.
31. **Remick, D. G., G. R. Bolgos, J. Siddiqui, J. Shin, and J. A. Nemzek.** 2002. Six at six: interleukin-6 measured 6 h after the initiation of sepsis predicts mortality over 3 days. Shock **17:**463–467.
32. **Ritchie, J. M., C. M. Thorpe, A. B. Rogers, and M. K. Waldor.** 2003. Critical roles for stx2, eae, and tir in enterohemorrhagic Escherichia coli-induced diarrhea and intestinal inflammation in infant rabbits. Infect. Immun. **71:**7129–7139.
33. **Romer, W., L. Berland, V. Chambon, K. Gaus, B. Windschiegl, D. Tenza, M. R. Aly, V. Fraisier, J. C. Florent, D. Perrais, C. Lamaze, G. Raposo, C. Steinem, P. Sens, P. Bassereau, and L. Johannes.** 2007. Shiga toxin induces tubular membrane invaginations for its uptake into cells. Nature **450:**670–675.
34. **Rutjes, N. W., B. A. Binnington, C. R. Smith, M. D. Maloney, and C. A. Lingwood.** 2002. Differential tissue targeting and pathogenesis of verotoxins 1 and 2 in the mouse animal model. Kidney Int. **62:**832–845.
35. **Sakiri, R., B. Ramegowda, and V. L. Tesh.** 1998. Shiga toxin type 1 activates tumor necrosis factor-alpha gene transcription and nuclear translocation of the transcriptional activators nuclear factor-kappaB and activator protein-1. Blood **92:**558–566.

36. **Sauter, K. A. D., A. R. Melton-Celsa, K. Larkin, M. L. Troxell, A. D. O'Brien, and B. E. Magun.** 2008. Mouse model of hemolytic-uremic syndrome caused by endotoxin-free Shiga toxin 2 (Stx2) and protection from lethal outcome by anti-Stx2 antibody. Infect. Immun. **76:**4469–4478.

37. **Sheoran, A. S., S. Chapman-Bonofiglio, B. R. Harvey, J. Mukherjee, G. Georgiou, A. Donohue-Rolfe, and S. Tzipori.** 2005. Human antibody against Shiga toxin 2 administered to piglets after the onset of diarrhea due to Escherichia coli O157:H7 prevents fatal systemic complications. Infect. Immun. **73:**4607–4613.

38. **Siegler, R. L., T. G. Obrig, T. J. Pysher, V. L. Tesh, N. D. Denkers, and F. B. Taylor.** 2003. Response to Shiga toxin 1 and 2 in a baboon model of hemolytic uremic syndrome. Pediatr. Nephrol. **18:**92–96.

39. **Siegler, R. L., T. J. Pysher, R. Lou, V. L. Tesh, and F. B. Taylor, Jr.** 2001. Response to Shiga toxin-1, with and without lipopolysaccharide, in a primate model of hemolytic uremic syndrome. Am. J. Nephrol. **21:**420–425.

40. **Siegler, R. L., T. J. Pysher, V. L. Tesh, and F. B. Taylor, Jr.** 2001. Response to single and divided doses of Shiga toxin-1 in a primate model of hemolytic uremic syndrome. J. Am. Soc. Nephrol. **12:**1458–1467.

41. **Smith, W. E., A. V. Kane, S. T. Campbell, D. W. K. Acheson, B. H. Cochran, and C. M. Thorpe.** 2003. Shiga toxin 1 triggers a ribotoxic stress response leading to p38 and JNK activation and induction of apoptosis in intestinal epithelial cells. Infect. Immun. **71:**1497–1504.

42. **Stearns-Kurosawa, D. J., F. Lupu, F. B. Taylor, Jr., G. Kinasewitz, and S. Kurosawa.** 2006. Sepsis and pathophysiology of anthrax in a nonhuman primate model. Am. J. Pathol. **169:**433–444.

43. **Tam, P. J., and C. A. Lingwood.** 2007. Membrane cytosolic translocation of verotoxin A1 subunit in target cells. Microbiology **153:**2700–2710.

44. **Taylor, F. B., Jr., V. L. Tesh, L. DeBault, A. Li, A. C. Chang, S. D. Kosanke, T. J. Pysher, and R. L. Siegler.** 1999. Characterization of the baboon responses to Shiga-like toxin: descriptive study of a new primate model of toxic responses to Stx-1. Am. J. Pathol. **154:**1285–1299.

45. **Tesh, V. L., J. A. Burris, J. W. Owens, V. M. Gordon, E. A. Wadolkowski, A. D. O'Brien, and J. E. Samuel.** 1993. Comparison of the relative toxicities of Shiga-like toxins type I and type II for mice. Infect. Immun. **61:**3392–3402.

46. **Torgersen, M. L., S. U. Lauvrak, and K. Sandvig.** 2005. The A-subunit of surface-bound Shiga toxin stimulates clathrin-dependent uptake of the toxin. FEBS J. **272:**4103–4113.

47. **Wong, C. S., S. Jelacic, R. L. Habeeb, S. L. Watkins, and P. I. Tarr.** 2000. The risk of the hemolytic-uremic syndrome after antibiotic treatment of Escherichia coli O157:H7 infections. N. Engl. J. Med. **342:**1930–1936.

Editor: B. A. McCormick